

## Characterization of the brittleness of hard rock at different temperatures using uniaxial compression tests

Guoqing Chen<sup>\*1,2</sup>, Tianbin Li<sup>1</sup>, Wei Wang<sup>1</sup>, Fan Guo<sup>1</sup> and Hongyu Yin<sup>1</sup>

<sup>1</sup> State Key Laboratory of Geohazard Prevention and Geoenvironment Protection, Chengdu University of Technology, #1 Dongsanlu, Erxianqiao, Chengdu 610059, Sichuan, China

<sup>2</sup> State Key Laboratory of Geomechanics and Geotechnical Engineering, Institute of Rock and Soil Mechanics, Chinese Academy of Sciences, Wuhan, Hubei 430071, China

(Received March 08, 2016, Revised January 11, 2017, Accepted February 16, 2017)

**Abstract.** The failure mechanism of a deep hard rock tunnel under high geostress and high geothermal activity is extremely complex. Uniaxial compression tests of granite at different temperatures were conducted. The complete stress-strain curves, mechanical parameters and macroscopic failure types of the rock were analyzed in detail. The brittleness index, which represents the possibility of a severe brittleness hazard, is proposed in this paper by comparing the peak stress and the expansion stress. The results show that the temperature range from 20 to 60°C is able to aggravate the brittle failure of hard rock based on the brittleness index. The closure of internal micro cracks by thermal stress can improve the strength of hard rock and the storage capacity of elastic strain energy. The failure mode of the samples changes from shear failure to tensile failure as the temperature increases. In conclusion, the brittle failure mechanism of hard rock under the action of thermal coupling is revealed, and the analysis result offers significant guidance for deep buried tunnels at high temperatures and under high geostress.

**Keywords:** deep buried tunnel; high geothermal activity; brittle failure; expansion stress

### 1. Introduction

Due to the needs of engineering construction and human activities, many deep buried tunnels pass through complex nontectonic and geothermally active zones. Deep hard rock tunnels are affected by not only brittle bursting hazards under the action of high geostress (Chen *et al.* 2013, Feng and Hudson 2011, Li *et al.* 2012, Zhang *et al.* 2012) but also by high geothermal hazards (Rybach and Pfister 1994, Wilhelm and Rybach 2003). The mechanical properties of rock in a tunnel with high geothermal activity are affected by the temperature. High geostress and high geothermal activity increase the complexity of the rock's failure mechanism.

The Anfang tunnel in Japan (maximum depth of 700 m and ground temperature of 75°C, Chen *et al.* 2014), the Simplon tunnel in Switzerland (maximum depth of 2,140 m and ground temperature of 55°C, Toula 1917, Rybach and Pfister 1994), the Lotschberg and Gotthard tunnel (Wilhelm and Rybach 2003), and the Maurienne-Ambin tunnel (Goy *et al.* 1996) all have high geothermal activity. Additionally, in the Gaoligong tunnel in Yunnan of China, the maximum principal stress is as high as 50 MPa, and the ground temperature of the surrounding rock can

---

\*Corresponding author, Professor, E-mail: [chgq1982@126.com](mailto:chgq1982@126.com)

reach 70°C. Therefore, the Gaoligong tunnel suffers greatly from bursting and thermo-mechanical coupling. The mechanical behavior of the rock in environments with high geostresses and high geothermal activity must be studied further to understand deep hard rock tunnels.

In studies of the brittle failure of hard rock, some indexes have been proposed to describe the characteristics of rockbursts; these include the stress index (Eberhardt *et al.* 1998, Martin 1993, Meng *et al.* 2015, Singh 1987), the damage factor of the uniaxial compression strength (Diederichs *et al.* 2004, Shen *et al.* 2014) and the energy index (Jiang *et al.* 2010, 2013). However, these indexes do not consider the temperature.

In studies of thermal coupling in rock, Alm (1985), Brede and Haasen (1988), Wan *et al.* (2009), Yavuz *et al.* (2010), Ranjith *et al.* (2012), Wisetsaen *et al.* (2015) and Liu and Xu (2015) researched the mechanical characteristics of rock at high temperatures and high stresses. David *et al.* (1999), Pan *et al.* (2009), Zhou *et al.* (2011), Koyama *et al.* (2013), Jiao *et al.* (2015) and Amarasiri and Kodikara (2015) studied thermal cracking in hard rock. However, few studies have considered the effect of the temperature on the brittleness of hard rock.

A considerable amount of research has focused on the thermal coupling of rock mechanics and brittle failure in the form of bursting, but the mechanism underlying the brittleness of hard rock in environments with high geothermal activity has not been revealed. Therefore, in this paper, uniaxial compression tests were conducted at different temperatures to study the brittleness mechanism of hard rock under the action of thermal coupling. The results show that increasing the temperature aggravates the brittle failure of hard rock. Additionally, the analysis results contribute to our understanding of the failure of deep tunnels in response to high geostress and high geothermal activity.

## 2. Materials and methods

### 2.1 Materials

The Gaoligong mountain area of the Dali-Ruili Railway is located on the Yunnan-Burma and Thailand-Asia plate near the collision suture zone of the Indian and Eurasian plates, as shown in Fig. 1. The geostress in this area is high because of the intensive collision and compression of the two plates. Therefore, its geological engineering characteristics include complex structures, intense neotectonism, high geothermal activity and high geostress.

The region through which the Dali-Ruili Railway passes contains a variety of magmatic rocks (e.g., granite, diorite, gabbro and basalt) of different ages. Severe brittle failure, such as bursting and spalling, can be caused by high geostress in an area with hard rock. Additionally, the surrounding rock fails, a process that is more complex in an environment with a high geothermal activity. Therefore, the probability of bursting should be investigated based on the effects of the high geostress and high geothermal activity conditions.

The rock samples used in the study are biotitic granite, and the fabricated precision of the samples was in accordance with the standard of the International Society for Rock Mechanics. The samples were formed into cylinders. The height was 10 cm (with an accuracy of 1 mm), and the diameter was 5 cm. The ends, which were vertical relative to the axis of the sample, were parallel to within 0.02 mm, and the deviation between each end and the axis was less than 0.2°. In addition, the bearing frame and the diameter of the sample were of the same size to avoid errors in the compressive strength measurements.

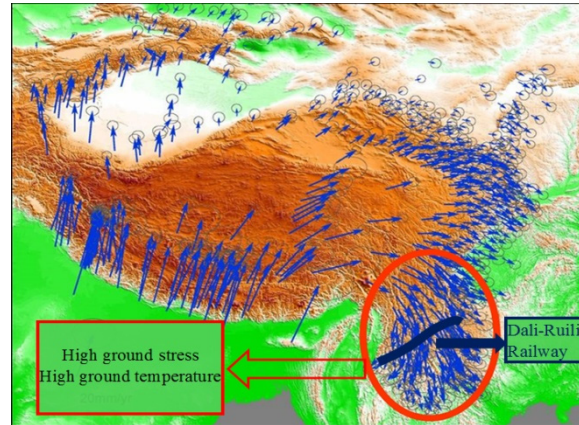


Fig. 1 Regional geological background of the Dali-Ruili Railway



(a)



(b)

Fig. 2 MTS 815 test system

## 2.2 Methods

Uniaxial compression tests of the rock were performed under unconfined conditions. The stress-strain process included an initial loading stage, a linear elastic stage, an obvious crack stage, a peak compressive strength stage, and a post-peak stage in which stress decreases significantly. The axial and lateral deformations of the sample were tested throughout the stress-strain process.

A thermal rigidity servo testing machine (an MTS815 test system) was employed in the uniaxial compression tests of the granite samples (Fig. 2). The temperature range of the MTS is from room temperature to 200°C. The MTS system can track the overall process of rock failure and the full stress-strain curve of rock at different temperatures because of its good dynamics and static stiffness.

The test temperature could be fixed at five levels: 20, 40, 60, 90 and 130°C. The heating equipment in the uniaxial test was a DHG-9203 electro-thermostatic blast oven (Fig. 3). The temperature was held constant for 2 h after it reached the set temperature. The loading rate was controlled at an axial displacement rate of 0.1 mm/min in the elastic deformation stage and then, by a lateral deformation rate of 0.03 mm/min until ultimate failure, when the sample entered the failure stage.



Fig. 3 Heating equipment

Table 1 Physical properties and the temperature setup of the samples for uniaxial compression testing

No.	Diameter × Height (mm)	Density (g/cm <sup>3</sup> )	Temperature (°C)
A-20	51.0 × 98.7	2.6	20
B-20	50.9 × 99.8	2.6	20
C-20	50.8 × 99.1	2.7	20
A-40	50.7 × 99.4	2.6	40
B-40	50.7 × 99.6	2.6	40
C-40	50.7 × 99.1	2.7	40
D-40	50.9 × 99.6	2.7	40
A-60	50.8 × 99.3	2.7	60
B-60	50.7 × 99.3	2.7	60
C-60	50.9 × 100.0	2.6	60
A-90	50.7 × 99.4	2.6	90
B-90	50.8 × 100.0	2.7	90
C-90	51.0 × 99.1	2.7	90
A-130	50.7 × 99.8	2.7	130
B-130	50.8 × 98.9	2.7	130
C-130	50.9 × 99.5	2.6	130
D-130	50.7 × 99.7	2.6	130

The complete stress-strain curve was measured, enabling the calculation of the uniaxial compressive strength, residual strength, Young's modulus and Poisson's ratio at different temperatures. The physical properties and the temperature setup are shown in Table 1.

### 2.3 Testing program

#### 2.3.1 Stress-strain characteristics

The axial strain, lateral strain and volumetric strain were analyzed as functions of the axial load. Crack initiation, damage and propagation during the progressive failure of hard rock can be

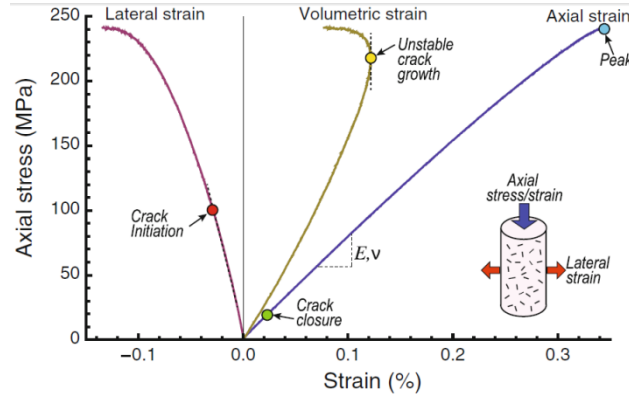


Fig. 4 Typical stress-strain response recorded in a uniaxial compressive test (Nicksiar and Martin 2012)

identified using three curves (Nicksiar and Martin 2012). As shown in Fig. 4, the volumetric strain can be determined as follows

$$\varepsilon_v = \varepsilon_1 + 2\varepsilon_3 \quad (1)$$

where  $\varepsilon_v$  is the volumetric strain,  $\varepsilon_1$  is the axial strain, and  $\varepsilon_3$  is the lateral strain.

### 2.3.2 Mechanical parameters

The unconfined compression test was used to quickly obtain the approximate strength of rock samples. The unconfined compressive strength (UCS), Young's modulus and Poisson's ratio were calculated in this study. The UCS was taken as the peak stress with the corresponding axial strain at failure in the stress-strain curve. The Young's modulus ( $E$ ) and Poisson's ratio ( $\mu$ ) were calculated as follows

$$E_{50} = \frac{\sigma_{50}}{\varepsilon_{L50}} \quad (2)$$

where  $E_{50}$  is the Young's modulus of the rock (GPa),  $\sigma_{50}$  is the stress at 50% of the peak, and  $\varepsilon_{L50}$  is the strain in the longitudinal direction when the stress is  $\sigma_{50}$ , and

$$\mu_{50} = \frac{\varepsilon_{d50}}{\varepsilon_{L50}} \quad (3)$$

where  $\mu_{50}$  is the Poisson's ratio,  $\varepsilon_{L50}$  is the axial strain corresponding to  $\sigma_{50}$  and  $\varepsilon_{d50}$  is the circumferential strain corresponding to  $\sigma_{50}$ . The axial and circumferential strains are assumed to be compressive and tensile, respectively.

### 2.3.3 Brittleness index for the probability of bursting

An investigation of the mechanism underlying a rockburst should consider the structure of the rock mass, variations in the ground stress and other more complex factors. However, this paper only considers the role of temperature and studies the effect of temperature on rockbursts. Therefore, the test has been performed at different temperatures. The progressive failure of hard rock includes three key stresses: the crack initiation stress,  $\sigma_{ci}$ , the volume expansion stress,  $\sigma_{cd}$  (i.e., the onset of unstable crack growth), and the peak stress,  $\sigma_f$ . It has been shown that the stress-

strain curve indicates different initial, expansion and peak stresses at different temperatures. However, taken together, the influence of temperature is most significant on the mechanical properties of the sample during unstable crack growth and on the peak stress. Therefore, the expansion stress and the peak stress index are determined to reflect the influence of the temperature on the brittleness of the rock.

In addition, the value of  $\sigma_{cd}$  can be easily obtained because it corresponds to the maximum volumetric strain on the volumetric strain curve (see Fig. 4). Expansion of the rock indicates the onset of failure, and the relatively early appearance of  $\sigma_{cd}$  can drive crack growth and energy dissipation. Finally, this paper proposes another brittleness index for hard rock that includes the possibility of brittle failure. The brittleness index is denoted by  $P_R$ . A higher value of  $P_R$  indicates a higher possibility of bursting.  $P_R$  is calculated as follows

$$P_R = \frac{\sigma_{cd}}{\sigma_f} \quad (4)$$

where  $P_R$  indicates the probability of bursting,  $\sigma_f$  is the peak stress and  $\sigma_{cd}$  is the expansion stress.

A smaller value of  $\sigma_{cd}$  indicates greater crack penetration and more dissipated energy. The final amount of energy released is small after the peak strength,  $\sigma_f$ , is reached, and the degree of brittle failure is small. In contrast, there is no crack growth or energy dissipation in the rock when  $\sigma_{cd}$  is close to  $\sigma_f$ , which causes a large amount of energy to be released and ensures that the rock's failure is intense. In other words, the rock is more likely to burst.

### 3. Results and discussion

#### 3.1 Stress-strain characteristics

Fig. 5 shows several stress-strain relationships, including axial stress-axial strain, axial stress-lateral strain and axial stress-volume strain at different temperatures. The decrease in stress after the peak is rapid at 20, 40 and 60°C. The brittle failure characteristic appears in the granite when

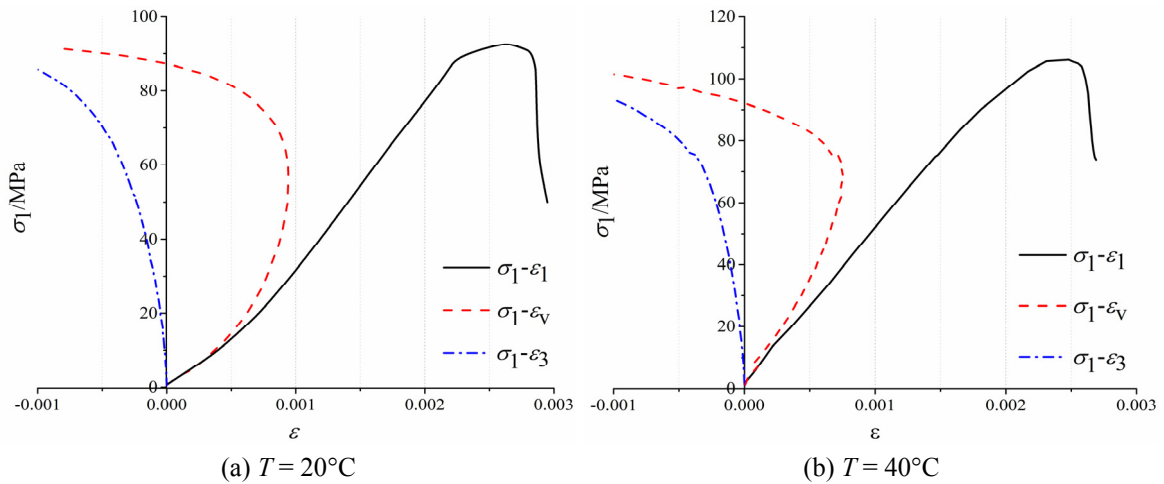


Fig. 5 Three stress-strain curves at different temperatures (compression is positive; dilation is negative)

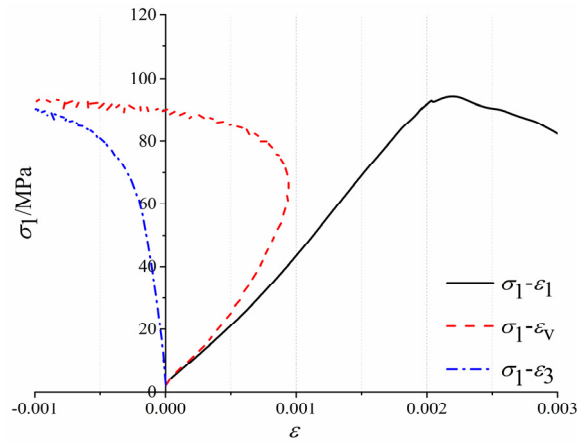
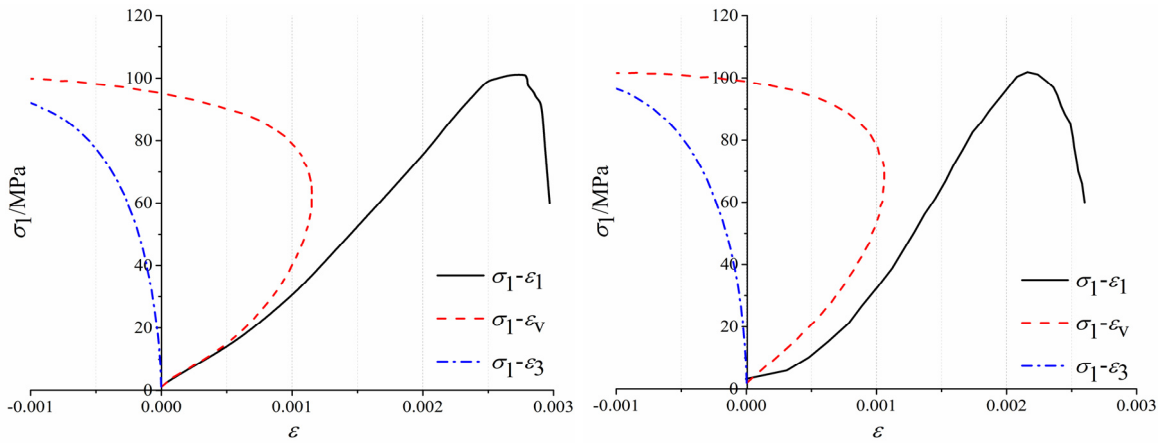


Fig. 5 Continued

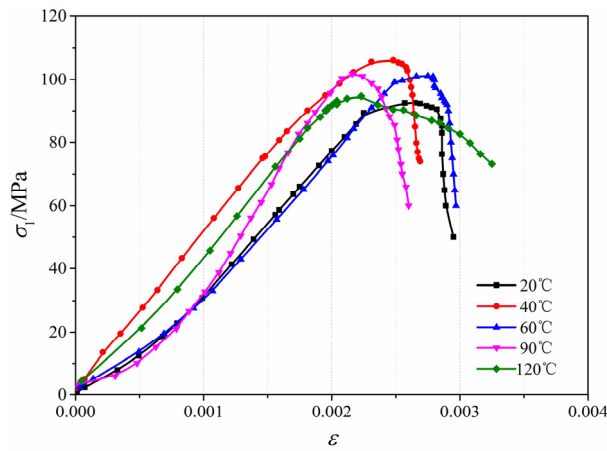


Fig. 6 Uniaxial stress-strain curves for different temperatures

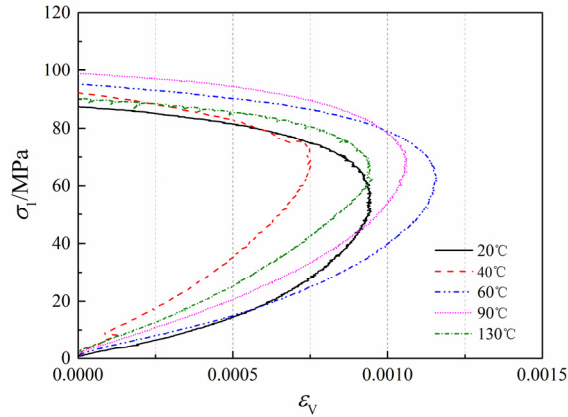


Fig. 7 Volumetric strain as a function of temperature

the temperature is between 20°C and 60°C. Therefore, granite exhibits a tendency to burst in this experimental temperature range. The reason for this tendency is that the temperature influences the capacity for storing elastic strain energy and the stress environment.

The type of failure changes from brittle to ductile at higher temperatures. Samples heated to higher temperatures and compressed uniaxially deformed in a plastic manner, as did sandstone at temperatures between 400°C and 950°C (Ranjith *et al.* 2012), mudstone between 600°C and 800°C (Zhang *et al.* 2014), granite between 400°C and 800°C (Chen *et al.* 2012), limestone between 400°C and 600°C (Syała *et al.* 2013), and marble at temperatures above 800°C (Zhang *et al.* 2009). However, it is nearly impossible for the temperature of a tunnel with high geothermal activity to exceed 100°C, and the brittle failure characteristic is clearly observed between room temperature and 100°C.

Fig. 6 also shows axial stress-axial strain curves at different temperatures to examine the UCS, Young's modulus ( $E$ ) and Poisson's ratio ( $\mu$ ). Before failure, the curves differ somewhat in shape and show considerable elastic deformation. After failure, the brittle deformation decreases sharply, except at 120°C.

The dependence of the volumetric strain on the temperature is shown in Fig. 7. It can be seen that the volume expansion stress,  $\sigma_{cd}$ , decreases significantly when the temperature is between 20°C and 40°C and then increases gradually as the temperature increases.

### 3.2 Mechanical parameters

Three samples were used for each temperature. The granite samples were collected from the same block of rock in the Gaoligong mountains. Therefore, the homogeneity of the samples is guaranteed, and the differences in the physical parameters between the samples are small. The unique variable of the test is temperature, and only its effect on the on mechanical properties of the sample is considered; the other conditions, such as the lithology and continuity of the sample, are kept constant. Therefore, only the standard stress-strain curve for each temperature is shown in Fig. 7; the other curves are shown in the Appendix. The UCS,  $E$ ,  $\mu$  and  $\sigma_{cd}$  can be calculated using the above mentioned stress-strain curves and equations. The test results are shown in Table 2. Small changes in various parameters of the samples were found at a constant temperature; they are shown in Table 2.

Table 2 Uniaxial compressive test results

No.	UCS (MPa)	Average UCS (MPa)	$E$	Average $E$	$\mu$	Average $\mu$	$\sigma_{cd}$ (MPa)	Average $\sigma_{cd}$ (MPa)
A-20	92.86		34.8		0.154		39.09	
B-20	93.87	92.93	34.2	34.53	0.157	0.155	39.88	39.26
C-20	92.06		34.6		0.153		38.80	
A-40	106.82		52.2		0.146		65.15	
B-40	106.23	107.62	51.4	52.67	0.149	0.146	66.10	65.22
D-40	109.80		54.4		0.144		64.40	
A-60	101.62		34.6		0.120		60.10	
B-60	101.16	101.34	34.1	34.13	0.125	0.124	59.92	60.02
C-60	101.24		33.7		0.127		60.05	
A-90	102.84		39.4		0.133		52.18	
B-90	103.21	102.94	39.7	38.77	0.131	0.132	51.83	52.17
C-90	102.76		37.2		0.131		52.51	
B-130	96.05		44.1		0.132		46.00	
C-130	95.73	96.38	43.9	43.40	0.131	0.132	45.90	45.86
D-130	97.36		42.2		0.132		45.69	

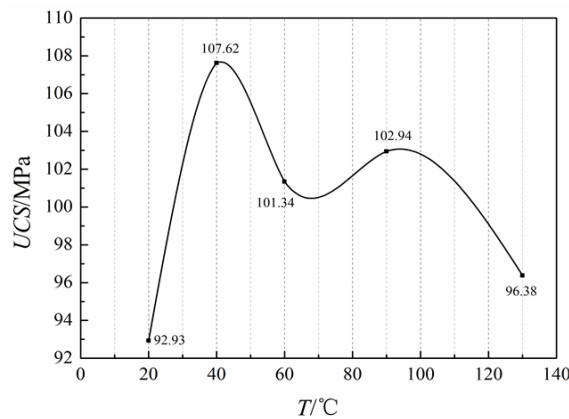


Fig. 8 UCS as a function of temperature

The dependence of the UCS on the temperature is shown in Fig. 8.

The UCS first increases and then decreases as the temperature increases. Its value increases by 15.54% between 20°C and 40°C and then decreases by 4.67%, 3.74%, and 10.28%, at 60, 90 and 130°C, respectively, in comparison with its value at 40°C. The decrement from 60°C to 130°C gradually increases.

According to the above analysis, the UCS reaches its maximum at 40°C. The thermal expansion of the minerals inside the rock results in partial closure of the original crack. Therefore, the stiffness and strength increase at 40°C in response to increased temperature. The rock's strength may decrease as the temperature increases if the sample is heated to 1,000°C. However,

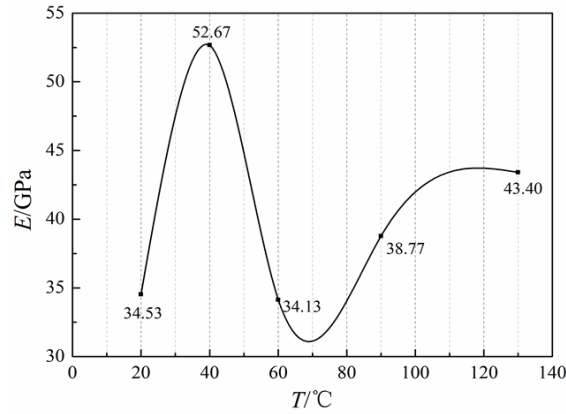


Fig. 9 Young's modulus as a function of temperature

there is a threshold temperature such that the UCS increases with the temperature when the temperature is below the threshold and decreases as the temperature increases when the temperature is above the threshold. The threshold is different for different rocks. The thresholds for marble, sandstone, mudstone and sand slate are 100, 400, 600 and 1,000°C, respectively (Sygala *et al.* 2013). In this paper, the UCS of granite changes slightly and reaches its maximum at 40°C. This result shows that the temperature range of 20-60°C is able to increase the UCS and aggravate the brittle failure of hard rock. Moreover, the phase transition temperature of quartz, which is the major constituent of granite, is 573°C (Chen *et al.* 2012). Therefore, the basic physical and mechanical characteristics of the minerals in granite do not change when the temperature is considerably below 573°C.

The dependence of Young's modulus on the temperature is shown in Fig. 9.

The general trend of the Young's modulus is to increase, decrease and then increase as the temperature increases (Fig. 9). The Young's modulus increases by 18.14 GPa between 20°C and 40°C and then decreases by 18.54 GPa between 40°C and 60°C. Additionally, the Young's modulus increases by 4.64 GPa between 60°C and 90°C and then by 4.63 GPa between 90°C and 130°C.

The Young's modulus increases considerably when the temperature reaches 40°C. This is probably because the rock's mineral crystals expand considerably at this temperature due to thermal action and the closure of internal micro cracks. Therefore, the ability to resist deformation increases, which increases Young's modulus. The internal crystals of the rock continue to expand as the temperature increases, resulting in new cracks and decreasing Young's modulus.

The measured values of Poisson's ratio as a function of temperature are shown in Fig. 10.

The general trend of Poisson's ratio is to decrease and then increase as the temperature increases (Fig. 10). It can be found that Poisson's ratio reaches its minimum at 60°C because the rock's mineral crystals expand considerably at this temperature. However, Poisson's ratio increases after reaching its minimum because the internal structure, water content and porosity of the rock change as the temperature increases.

The deformation of a rock determined by Young's modulus and Poisson's ratio depends mainly on the stiffness of the minerals that comprise it and the density, moisture and porosity. The Young's modulus increases by 34%, 50% and 60% at 40°C compared with its value at room temperature for the two types of sandstone and mudstone (Sygala *et al.* 2013). The changes in the Young's modulus and the UCS exhibit the same characteristics at different temperatures.

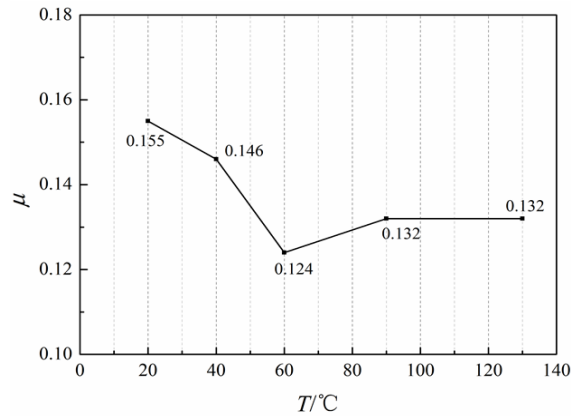


Fig. 10 Poisson's ratio as a function of temperature

### 3.3 Brittleness index for the possibility of bursting

The brittle failure of rock is a gradual process: in the first stage, the original crack closes, and then, a new crack develops stably; in the second stage, connection, penetration, intersection, shear sliding or splitting of the crack occurs; finally, macroscopic shear or a split fractured face is formed, and the rock fails.

The initiation stress,  $\sigma_{ci}$ , is often used to estimate the brittleness mechanisms of rock (Cai *et al.* 2004, Martin 1993). The brittleness of different types of rock with different mineral compositions and different grain sizes is estimated effectively by  $\sigma_{ci}$  (Martin 1993, Xue *et al.* 2014). However, the initiation stress,  $\sigma_{ci}$ , is difficult to obtain by acoustic emission and other methods (Liu *et al.* 2014). Furthermore, the difference in  $\sigma_{ci}$  is small for a given rock at different temperatures. Therefore, the expansion stress,  $\sigma_{cd}$ , is another feasible index for estimating the brittleness of hard rock (Xue *et al.* 2014). It can also be used to identify the brittleness mechanisms of a given rock at different temperatures.

The expansion stress,  $\sigma_{cd}$ , is also called the initial point of unsteady growth of a crack. It is also known as the damage strength, which increases damage to the internal rock. Thereafter, the cracks begin to connect and intersect, and the rock enters the apparent expansion stage. The crack growth process is continuously unsteady until failure when the stress applied to the rock is larger than  $\sigma_{cd}$ , even if it is constant. From an energy standpoint, the internal elastic strain energy is rapidly released during penetration of the fracture surface once the stress reaches the peak strength. The cracks in the rock begin to penetrate, causing the release of cumulative strain energy, when the stress applied to the rock is greater than  $\sigma_{cd}$ . If the expansion stress appears at an early stage (when  $\sigma_{cd}$  is small), then, the energy dissipation is high before the peak strength is reached, and the final released energy decreases after the peak strength is reached.

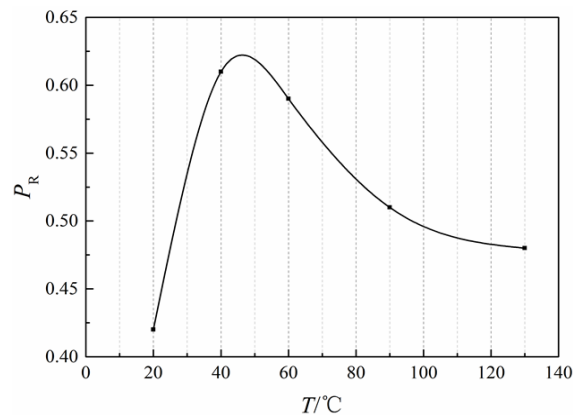
Therefore,  $P_R$  can be calculated using Table 2 and Eq. (4), and the results are shown in Table 3.

$P_R$  first increases from 20°C to 40°C and then decreases when the temperature exceeds 40°C (Fig. 11). The maximum of  $P_R$  is between 40°C and 60°C. In other words, the possibility of bursting and brittle failure is higher in this temperature range. Chen *et al.* (2014) found similar characteristics for brittle rock at different temperatures. The brittle failure of Äspö diorite was aggravated by heated thermal loading in an Äspö pillar (Koyama *et al.* 2013).

The dependence of  $P_R$  on the temperature is shown in Fig. 11.

Table 3  $P_R$  at different temperatures

Temperature	Peak stress $\sigma_f$ (MPa)	Expansion stress $\sigma_{cd}$ (MPa)	$P_R$
20°C	92.93	39.26	0.42
40°C	107.62	65.22	0.61
60°C	101.34	60.02	0.59
90°C	102.94	52.17	0.51
130°C	96.38	45.86	0.48

Fig. 11  $P_R$  as a function of temperature

The uniaxial compression failure mechanism is related to mineral components of biotite granite, such as hornblende, quartz, feldspar, and mica, under the action of temperature. The physical and mechanical properties and cementing form of the mineral components are altered as the temperature increases. The crack closure behavior during compression is an intrinsic property of the hard rock (Peng *et al.* 2015). Thermal stress is produced between the mineral grains, causing volume transformation of the interior minerals and closure of the original micro cracks.

### 3.4 Failure characteristics

Failure models of rock samples at different temperatures are shown in Fig. 12. In general, shear and tensile failure are observed in the uniaxial compressive test. Shear failure occurs mainly at 20°C, and tensile failure occurs between 40°C and 130°C. The failure models of biotitic granite with a tendency to burst transition from shear failure to tensile failure as the temperature increases under unidirectional stress.

New micro cracks are generated as particles separate and the tensile strength decreases as the temperature increases continuously. The tensile strength of the samples is weakened by thermal action under axial loading, and fissures develop parallel to the axial force. The test results show that the type of failure changes from shear failure to tensile failure because of the increasing temperature. The change in the failure mode, which can be distinguished quantitatively by monitoring using an acoustic emission or a high-speed camera from a microscopic perspective, can be easily observed in the failed samples at different temperatures. Microscopic monitoring of the failure processes of samples will be included in future tests.

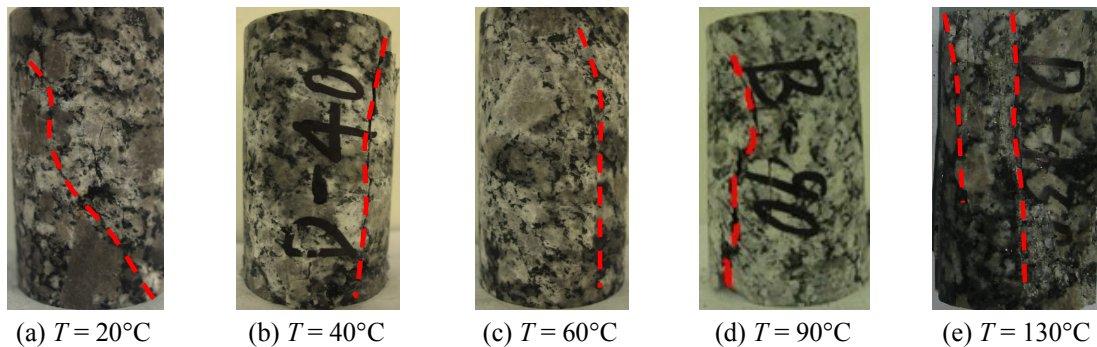


Fig. 12 Shear and tensile failure with increasing temperature

#### 4. Conclusions

The basic mechanical parameters of rock at high temperatures have been widely studied. The strength of rock generally decreases as the temperature increases. However, no quantitative assessment of brittleness is available for hard rock at different temperatures. This study proposes a brittleness index, and the brittleness of granite is found to be strengthened by thermal loading at temperatures ranging between 20°C and 60°C.

- The thermal stress caused by the thermal load affects internal micro cracks and changes the brittleness of the hard rock. The UCS and the Young's modulus increase at 40°C because of the closure of internal micro cracks. Therefore, increasing the temperature within the range from 20 to 60°C increases the strength of granite.
- The volumetric strain and expansion points also represent the failure of hard rock.  $P_R$ , which represents the probability of brittle failure, is proposed for the same rock at different temperatures in this paper. The maximum values of  $P_R$  occurs at 40°C and 60°C. Bursting is more likely in tunnels where the surrounding rock is between 20°C and 60°C.
- The tensile strength is decreased by thermal action under axial loading, and fissures develop parallel to the axial force. The type of failure changes from shear to tensile as the temperature increases.

#### Acknowledgments

This work is supported by the National Natural Science Foundation of China under grant nos. 41230635 and 41572283. Thanks are given for funding by the Science and Technology Office of Sichuan Province (grant no. 2015JQ0020). This work is also supported by the Open Research Fund of the State Key Laboratory of Geomechanics and Geotechnical Engineering, Institute of Rock and Soil Mechanics, Chinese Academy of Sciences under grant no. Z014008.

#### References

- Alm, O. (1985), "The influence of micro crack density on the elastic and fracture mechanical properties of stropa granite", *Phys. Earth Planet. Inter.*, **30**(40), 161-179.
- Amarasiri, A.L. and Kodikara, J.K. (2015), "Effect of characteristic lengths of fracture on thermal crack

- patterns”, *Int. J. Geomech.*, **15**(4), 04014071.
- Brede, M. and Haasen, P. (1988), “The brittle-to-ductile transition in doped silicon as a model substance”, *Acta Metall.*, **36**(8), 2003-2018.
- Cai, M., Kaiser, P.K., Tasaka, Y., Maejima, T., Morioka, H. and Minami, M. (2004), “Generalized crack initiation and crack damage stress thresholds of brittle rock masses near underground excavations”, *Int. J. Rock Mech. Min. Sci.*, **41**(5), 833-847.
- Chen, Y.L., Ni, J., Shao, W. and Azzam, R. (2012), “An experimental study on the influence of temperature on the mechanical properties of granite under a uniaxial compression and fatigue loading”, *Int. J. Rock Mech. Min. Sci.*, **56**(12), 62-66.
- Chen, G.Q., Li, T.B., Gao, M.B., Chen, Z.Q. and Xiang, T.B. (2013), “Deformation warning and dynamic control of dangerous disaster for Large Underground Caverns”, *Disaster Adv.*, **6**(s1), 422-430.
- Chen, G., Li, T., Zhang, G., Yin, H. and Zhang, H. (2014), “Temperature effect of rock burst for hard rock in deep-buried tunnel”, *Nat. Haz.*, **72**(2), 915-926.
- David, C., Menéndez, B. and Darot, M. (1999), “Influence of stress-induced and thermal cracking on physical properties and microstructure of La Peyratte granite”, *Int. J. Rock Mech. Min. Sci.*, **36**(4), 433-448.
- Diederichs, M.S., Kaiser, P.K. and Eberhardt, E. (2004), “Damage initiation and propagation in hard rock during tunnelling and the influence of near-face stress rotation”, *Int. J. Rock Mech. Min. Sci.*, **41**(5), 785-812.
- Eberhardt, E., Stead, D., Stimpson, B. and Read, R.S. (1998), “Identifying crack initiation and propagation thresholds in brittle rock”, *Can. Geotech. J.*, **35**(2), 222-233.
- Feng, X.T. and Hudson, J.A. (2011), *Rock Engineering Design*, CRC Press, Boca Raton, CA, USA.
- Goy, L., Fabre, D. and Menard, G. (1996), “Modelling of Rock Temperatures for Deep Alpine Tunnel Projects”, *Rock Mech. Rock Eng.*, **29**(1), 1-18.
- Jiang, Q., Feng, X.T., Xiang, T.B. and Su, G. (2010), “Rockburst characteristics and numerical simulation based on a new energy index: a case study of a tunnel at 2,500 m depth”, *Bull. Eng. Geol. Environ.*, **69**(3), 381-388.
- Jiang, Q., Feng, X.T., Chen, J., Huang, K. and Jiang, Y. (2013), “Estimating in-situ rock stress from spalling veins: A Case study”, *Eng. Geol.*, **152**(1), 38-47.
- Jiao, Y.Y., Zhang, X.L., Zhang, H.Q., Li, H., Yang, S. and Li, J. (2015), “A coupled thermo-mechanical discontinuum model for simulating rock cracking induced by temperature stresses”, *Comput. Geotechnics*, **67**, 142-149.
- Koyama, T., Chijimatsu, M., Shimizu, H., Nakama, S., Fujita, T., Kobayashi, A. and Ohnishi, Y. (2013), “Numerical modeling for the coupled thermo-mechanical processes and spalling phenomena in Aspo Pillar stability experiment (APSE)”, *J. Rock Mech. Geotechn. Eng.*, **5**(1), 58-72.
- Li, S.J., Feng, X.T., Li, Z.H., Chen, B., Zhang, C. and Zhou, H. (2012), “In situ monitoring of rockburst nucleation and evolution in the deeply buried tunnels of Jinping II hydropower station”, *Eng. Geol.*, **137-138**(6), 85-96.
- Liu, S. and Xu, J.Y. (2015), “An experimental study on the physico-mechanical properties of two post-high-temperature rocks”, *Eng. Geol.*, **185**, 63-70.
- Liu, J.P., Li, Y.H. and Xu, S.D. (2014), “Estimation of cracking and damage mechanisms of rock specimens with pre-cut holes by moment tensor analysis of acoustic emission”, *Int. J. Fract.*, **188**(1), 1-8.
- Martin, C.D. (1993), “The Strength of Massive Lac du Bonnet Granite around Underground Opening”, Ph.D. Dissertation; University of Manitoba, Manitoba Canada.
- Meng, F.Z., Zhou, H., Zhang, C.Q., Xu, R. and Lu, J. (2015), “Evaluation methodology of brittleness of rock based on post-peak stress-strain curves”, *Rock Mech. Rock Eng.*, **48**(5), 1787-1805.
- Nicksiar, M. and Martin, C.D. (2012), “Evaluation of methods for determining crack initiation in compression tests on low-porosity rocks”, *Rock Mech. Rock Eng.*, **45**(4), 607-617.
- Pan, P.Z., Feng, X.T., Huang, X.H., Cui, Q. and Zhou, H. (2009), “Coupled THM processes in EDZ of crystalline rocks using an elasto-plastic cellular automaton”, *Environ. Geol.*, **57**(6), 1299-1311.
- Peng, J., Rong, G., Cai, M. and Zhou, C. (2015), “A model for characterizing crack closure effect of rocks”,

- Eng. Geol.*, **189**, 48-57.
- Ranjith, P.G., Viete, D.R. and Chen, B.J. (2012), "Transformation plasticity and the effect of temperature on the mechanical behaviour of Hawkesbury sandstone at atmospheric pressure", *Eng. Geol.*, **151**(9), 120-127.
- Rybach, L. and Pfister, M. (1994), "How to predict rock temperatures for deep Alpine tunnels", *J. Appl. Geophys.*, **31**(1-4), 261-270.
- Shen, J.Y., Jimenez, R., Karakus, M. and Xu, C. (2014), "A simplified failure criterion for intact rocks based on rock type and uniaxial compressive strength", *Rock Mech. Rock Eng.*, **47**(2), 357-369.
- Singh, S.P. (1987), "The influence of rock properties on the occurrence and control of rockbursts", *Min. Sci. Technol.*, **5**(1), 11-18.
- Sygała, A., Bukowska, M. and Janoszek, T. (2013), "High temperature versus geomechanical parameters of selected rocks—the present state of research", *J. Sustainable Min.*, **12**(4), 45-51.
- Toula, F. (1917), "Geothermal conditions of the Simplon Mountains in the area of the great tunnel", *PetermannsMitteilungen*, **63**, 161-116.
- Wan, Z.J., Zhao, Y.S., Zhang, Y. and Wang, C. (2009), "Research status quo and prospection of mechanical characteristics of rock under high temperature and high pressure", *Procedia Earth Planet. Sci.*, **1**(1), 565-570.
- Wilhelm, J. and Rybach, L. (2003), "The geothermal potential of Swiss Alpine tunnels", *Geothermics*, **32**(4-6), 557-568.
- Wisetsaen, S., Walsri, C. and Fuenkajorn, K. (2015), "Effects of loading rate and temperature on tensile strength and deformation of rock salt", *Int. J. Rock Mech. Min. Sci.*, **73**, 10-14.
- Xue, L., Qin, S.Q., Sun, Q., Wang, Y., Lee, L.M. and Li, W. (2014), "A study on crack damage stress thresholds of different rock types based on uniaxial compression tests", *Rock Mech. Rock Eng.*, **47**(4), 1183-1195.
- Yavuz, H.S., Demirdag, S.C. and Caran, S. (2010), "Thermal effect on the physical properties of carbonate rocks", *Int. J. Rock Mech. Min. Sci.*, **47**(1), 94-103.
- Zhang, L.Y., Mao, X.B. and Lu, A. (2009), "Experimental study on the mechanical properties of rocks at high temperature", *Sci. China Ser. E-Technol. Sci.*, **52**(3), 641-646.
- Zhang, C.Q., Feng, X.T., Zhou, H., Qiu, S. and Wu, W. (2012), "Case histories of four extremely intense rockbursts in deep tunnels", *Rock Mech. Rock Eng.*, **45**(3), 275-288.
- Zhang, L.Y., Mao, X.B., Liu, R.X., Guo, X. and Ma, D. (2014), "The mechanical properties of mudstone at high temperatures: An experimental study", *Rock Mech. Rock Eng.*, **47**(4), 1479-1484.
- Zhou, H., Hu, D.W., Zhang, F.A. and Shao, J. (2011), "A thermo-plastic/viscoplastic damage model for geomaterials", *ActaMec. Solida Sin.*, **24**(3), 195-208.